Beetle exoskeleton may facilitate body heat acting differentially across the electromagnetic spectrum.

Luis M. Carrascal

Yolanda Jiménez Ruiz

Jorge M. Lobo*

Department of Biogeography and Global Change. Museo Nacional de Ciencias Naturales-C.S.I.C. C/ José Gutiérrez Abascal 2, 28002. Madrid, Spain.

Running head: heating capacity of beetle exoskeleton

*Corresponding author; e-mail: mcnj117@mncn.csic.es

Keywords: body position, dung beetles, exoskeleton, heating rates, interspecific differences, radiation source.

What is already known

- Limited and differing studies allow us to suggest that the exoskeleton of coleopteran may act as a structure capable of controlling body temperatures. However, we do not know of any study that specifically examines this question.

What this study adds

- The results provided by this study would constitute the first evidence supporting that beetle exoskeletons act differentially across the electromagnetic spectrum determining internal body temperatures.

ABSTRACT

Exoskeletons of beetles, and their associated morphological characteristics, can serve many different functions, including thermoregulation. We study the thermal role of the exoskeleton in 13 Geotrupidae dung beetle species using heating experiments under controlled conditions. The main purpose was to measure the influence of heating sources (solar radiance vs. infrared), animal position (dorsal vs. ventral exposure), species identity and phylogenetic relationships on internal asymptotic temperature and heating rates. The thermal response was significantly influenced by phylogenetic relatedness, although it was not affected by the apterous condition. The asymptotic internal temperature of specimens was not affected by the thoracic volume, but was significantly higher under simulated sunlight conditions than under infrared radiation, and when exposed dorsally as opposed to ventrally. There was, thus, a significant interaction between heating source and body position. Heating rate was negatively and significantly influenced by thoracic volume and, although insignificantly slower under simulated sunlight, it was significantly affected by body position, being faster under dorsal exposure. The results constitute the first evidence supporting the hypothesis that the beetle exoskeleton acts differentially across the electromagnetic spectrum determining internal body temperatures. This interesting finding suggests the existence of a kind of "passive physiology" imposed by the exoskeleton and body size, where interspecific relationships play a minor role.

Introduction

Exoskeletons of arthropods are composed of chitin and various proteins and waxes as basic materials, being one of the most resistant, ancestral, functionally versatile and abundant biomaterials (Gupta 2011). The evolution of the exoskeleton is key to the radiation of arthropods and the successful colonization of terrestrial environments by insects. Coleoptera constitutes the most diversified animal group on the Earth (Chapman 2009), in which the presence of protective sheathed wings (elytra) has become their main identifiable morphological characteristic.

The cuticle of beetles and their associated morphological characteristics are a continuous source of inspiration in biomimetics (Gorb 2013), because they can serve many different functions (physical barrier for internal tissues, attachment for muscles, food grinding, body cleaning, adhesion, sound generation, friction, lubrication, filtering, crypsis, mimicry, substrate matching, aposematism, sexual and visual signalling, thermoregulation, etc.). For some authors, the external characteristics of the insect cuticle as carinae, reticulations, macro and microsculptures are not the consequence of specific selective environmental forces acting evolutionarily (Ball 1985) or related to habitat differences (Doberski and Walmesley 2007). By contrast, other studies suggest that reticulation changes (Drotz et al. 2010) or thin patches (Slifer 1953) can be considered adaptations capable of controlling body temperature and thus affecting environmental performance. Cuticle darkness has been also associated with body temperature (Gross et al. 2004; Clusella Trullas et al. 2007; Schweiger & Beierkuhnlein 2016), management of UV-radiation (Mikhailov 2001), climatic changes (Davis et al. 2008; Zeuss et al. 2014) and immune response (Dubovskiy et al. 2013). Cold environmental conditions would promote the production of melanin in ectothermic species being this process related to the key role of the enzyme phenoloxidase in both

melanization and immune defense (the temperature-dependent immune physiological mechanism; see Fedorka et al. 2013). However, the association between immunity and cuticle darkness would not take place in Coleoptera because their colour variations are not pigmentary (Kinoshita 2008), but structural (i.e. due to the electron excitation by the incident light). The available studies in Geotrupidae dung beetles indicate that colour variations are due to simple multilayer reflectors (Pye, 2010; Akamine et al. 2011) and, as in other insect groups (Digby 1955; Umbers et al. 2013; Välimäki et al. 2015), there is no empirical evidence that supports the role of colour on heating differences and thermoregulation.

In this paper we study the thermal response to heat of the exoskeleton of the so called earth-boring dung beetle species (Geotrupidae). We study 13 geotrupid species broadly distributed throughout the phylogeny of the family using heating experiments under controlled conditions. The main purpose of this study is to measure the influence of heating sources (solar radiance vs. infrared), animal position (dorsal vs. ventral exposure) and species identity on heating rates, and to quantify the proportion of the observed variability attributable to those effects (Figure 1). Seven of these species have fully developed wings, while six are apterous (no wings) with the two elytra fused together (Table 1), an adaptation assumed to be directed to reduce water loss (but see Duncan 2002). The selected species also show slight differences in structural coloration (all are black) and surface reticulations and/or microsculptures. If interspecific differences in these traits are prominent for the acquisition of temperature in this group, we should expect a large proportion of variance in heating rates attributable to species identity under laboratory conditions. Moreover, these interspecific differences could be more notable under one of the two different sources of heat tested (simulated solar irradiance and infrared radiation), or considering the area of the animal being directly

affected (dorsal or ventral surface), illustrating potentially interesting interactions. It is reasonable to assume that the upper part of the beetle's exoskeleton mainly interacts with the range of wavelengths characterizing solar radiation, while the ventral part interacts primarily with the infrared radiation coming from the substrate. Thus, the comparison of the strikingly different smooth dorsal part and the complex and rough ventral texture (with setae and coxae, legs, etc.) would cast light on the importance of the exoskeleton surface in modulating heat rates. If present, a differential heat response between species would allow for further studies directed to identify the most probable characteristics of the exoskeleton responsible for these differences.

Material and Methods

Experimental conditions

Thirteen species of Palaearctic Geotrupidae were considered, all of them well distributed throughout the phylogenetic tree of this coleopteran family (Verdú et al. 2004; Cunha et al. 2011). For each one of these species, two specimens were selected from the insect collections available at the Museo Nacional de Ciencias Naturales (Madrid); specimens were dried from at least one year before. The selection of the two specimens was carried out in order to maximize the body size differences and location of origin between them when possible (Table 1).

Thorax length, width and thickness were measured in each specimen using an Olympus SC100 CMOS camera associated with a SZX10 stereo microscope. The thoracic pseudo-volume of each specimen was estimated as the corresponding one-fourth volume of the ellipsoid delimited by these three measurements, and used to assess the influence of animal size on the measured heating parameters (i.e., a larger

125 volume should require a longer time to reach the thermal asymptote, and smaller
126 animals heat faster).

127 Each specimen was finely holed in the apex of the pygidium using an
128 entomological pin, and a thin type-K thermocouple was inserted in this hole until its tip
129 reached the middle of the abdomen. The thermocouple wire was welded to the abdomen
130 using a small drop of hot thermoplastic glue. A Fluke 54 II B dual digital thermometer
131 (0.05% accuracy) was used for recording the internal temperature of each specimen at
132 ten seconds intervals during 8 minutes, except the first record that was measured at five
133 seconds since the beginning of the trial (49 temperature measurements in total).

134 Before each trial the specimen with the welded thermocouple was maintained in
135 a freezer until its internal temperature reached -5º C. The specimen was then placed in
136 the experimental arena, starting the recording of internal body temperatures (time 0)
137 when the temperature reached +5ºC. The so obtained body temperatures were
138 subsequently adjusted to the exponential function

139 $$\text{temperature (T)} = a * (b - exp(-c * \text{time}))$$

140 The product of *a* and *b* represents the asymptotic value at the end of the heating process,
141 while *c* measures the heating rate at the start of the recording process (i.e., heating
142 trials). Thus, the so obtained asymptotic values were positively correlated with the
143 temperature actually reached after eight minutes ($r = 0.9995$, $n=260$, $p < 0.001$; $T_{8\ min} =$
144 0.02+0.999*[a*b]); the *c* parameter was positively correlated with the increase in body
145 temperature 15 seconds after the beginning of the heating trial ($r = 0.882$, $n=260$, p
146 <0.001).

147 Temperature variations were recorded by submitting each specimen to two
148 different radiation sources (simulated solar radiance and infrared; SR and IF,
149 respectively) and two different body positions (dorsal or upside-up and ventral or

upside-down; D and V, respectively). The experimental specimens were placed 10 cm over the lab table, not being kept in contact with the substrata. Recall that we were interested in the direct influence of radiation sources on heating rates, thus avoiding the potential influence of other heat sources (e.g., conduction, thermal boundary layer, etc.). A 100 watts halogen neodymium lamp with a balanced daylight spectrum (from UVA to infrared radiations) was used to simulate natural sunlight conditions. A ceramic heat emitter of 150 watts was used to simulate long wavelength infrared emissions. These two radiation sources are frequently used in terrariophily to simulate natural sources of heat. The lamps were placed in the experimental arena at different heights above the experimental specimens, in order to match the air temperatures attained in the position of specimens subjected to heating. To control for subtle, random variations in the air temperature near the specimens, one thermocouple was located at 1 cm from the specimen and 10 cm over the lab table (T_{air}). This control temperature was used as a covariate to estimate and correct heating parameters independent of the temperature variations experienced during trials. The mean value (± 95% confidence interval) of T_{air} during the trials was 31.5 ± 0.3 ºC, being similar to those experienced by the species under Mediterranean natural conditions during summer at midday. In total, 260 assays were carried out (13 species x 2 specimens x 2 radiation sources x 2 body positions), repeating three times the temperature measurements of each specimen in dorsal position, and twice for ventral position, in order to obtain stabilized measurements (see Table 2); all trial replicates were conducted on different days.

This work conforms to the Spanish legal requirements including those relating to conservation and welfare.

Molecular analyses

175 Total DNA was extracted from frozen tissue with a DNA Easy extraction kit (Qiagen).
176 COI-Sca-Frevc (Lobo et al. 2015), HCO2198 (Folmer et al. 1994), C1-J-2183 (Simon et
177 al. 1994), COI-Sca-R, COIIam-Sca, and COIIB-605-Sca (Villalba et al. 2002) were the
178 primers used to amplify with PCR three overlapping fragments comprising the 3' end of
179 mitochondrial cytochrome oxidase I (COI), the adjacent complete tRNA-Leu (UUR),
180 and the 5' end of cytochrome oxidase II (COII) genes. A total of 40 PCR cycles
181 (denaturing at 94 ºC for 30 s, annealing at 42 ºC for 30 s, and extension at 72 ºC for 60
182 s) with an initial denaturing step at 94 ºC for 5 min, and a final extension step at 72 ºC
183 for 5 min, were performed to amplify the mitochondrial fragments. All PCR
184 amplifications were conducted in 25 µl reactions containing 3 mM $MgCl_2$, a 0.4 mM of
185 each dNTP, 0.2 µM of each primer, template DNA (10 to 100 ng), and DNA
186 polymerase (1 unit, Biotools). After PCR purification, samples were directly sequenced
187 using the corresponding PCR primers. Samples were sequenced in an automated DNA
188 sequencer (ABI PRISM 3700) using the Big-Dye Deoxy Terminator cycle-sequencing
189 kit (Applied Biosystems) following the manufacturer's instructions. Sequences were
190 deposited in EMBL under the accession numbers provided in Table 3.

191 DNA sequences were aligned with BioEdit v7.2.5 (Hall 1999) using the default
192 options. Both the Akaike (AIC) and the Bayesian (BIC) information criterion, as
193 implemented in jModelTest v2.1.7 (Darriba et al. 2012), selected GTR + I + G as the
194 evolutionary model that best fit the data. The selected evolutionary model and model
195 parameters (GTR + I + G; I = 0.503; G = 0.681) were used in the maximum likelihood
196 (ML) analysis performed with PhyML v.3.1 (Guindon et al. 2010). The robustness of
197 the inferred trees was tested by nonparametric bootstrapping (BP) using 1000
198 pseudoreplicates. Bayesian inference was also performed with MrBayes v.3.2.5
199 (Ronquist et al. 2012), running for 1 x 10^7 generations (four simultaneous Markov

chains; sample frequency 100). Four independent partitioned analyses were performed and checked for stationarity and convergence of the chains with Tracer v1.6 (Rambaut et al. 2013). Seven data partitions were analysed: mitochondrial COI gene (first, second, and third codon positions), mitochondrial COII gene (first, second, and third codon positions) and mitochondrial ARNtleu (uur) gene. Model parameters were estimated independently for each one of the respective data partitions. Burn-in was set to the first 1.000.000 generations. The robustness of the inferred Bayesian trees was determined using Bayesian posterior probabilities (BPP; as obtained from majority-rule consensus trees of the post burn-in trees). Two species of *Lethrus* (*Lethrus elephas* and *Lethrus perun*; Table 3) were selected as outgroups, based on a previous study (Cunha et al. 2011).

Statistical analyses

Non-linear regressions between temperature and time in each trial were carried out using CurveExpert 1.4 for Windows. The average explanatory capacity of the exponential regressions previously mentioned was 99.77% (95% confidence interval of R^2= 99.73 – 99.80 %).

Within-individual variation in heating parameters across trials was low (3 repetitions in the upside-up position, and two in upside-down position), accounting for a very small percentage of variance: 3.5% for asymptote and 4.9% for the increasing rate at the beginning of the heating experiments (nested ANOVA analyzing the residual variation of models that include the individuals nested within radiation sources and positions, divided by the total sum of squares). Therefore, the results obtained for the trials under the different experimental circumstances were very repeatable.

We used generalized linear mixed models (GLMM) to analyze the variation in the asymptote and the increasing rate at the beginning of the heating experiments (canonical distribution of the response variables: Gaussian; link functions: identity). The subtle variations in the temperature experienced during each heating trial (T_{air}) and the thoracic volume of the studied specimens were treated as fixed covariates, while the source of radiation (NS vs. IF), the body position (D vs. V) and species identity were considered as fixed factors. Specimen identity (two different individuals per species) was considered as a random factor. The GLMM also included all possible interactions among species, source and position (three two-way and one three-way). The mean square (*MS*) and the degrees of freedom (*df*) of the error terms were estimated following the Kenward & Roger method, which finds the linear combinations of sources of random variation that serve as appropriate error terms for testing the significance of the respective effect of interest (Kenward and Roger 1997). We used the R packages *lme4* and *lmerTest* (Kuznetsova et al. 2014; Bates et al. 2015) run under R version 3.1.2 (R Core Team 2014). The nested analyses of variance of the within-individual variation in heating parameters were carried out using the R command *aov{stats}*. In order to partition the variance according to the partial effects attributable to species, source of radiation, animal position and the two covariates, we built new mixed models deleting the interaction terms, and used the sum of squares of the marginal model.

It is commonly acknowledged that species are evolutionarily related throughout a phylogenetic scheme, and therefore they should not be treated as independent sample units in comparative analyses (Harvey and Purvis 1991; Rezende and Diniz-Filho 2012). Although this paper mainly deals with the biophysical response of beetle heating to sources of radiation and body position in 13 Geotrupidae species, we have also estimated the phylogenetic signal (Blomberg and Garland 2002) in interspecific

249 differences of the heating rate at the beginning of the experiments, and the asymptotic
250 internal temperature. The residuals of the linear mixed models (GLMM) were analyzed
251 onto the phylogenetic hypothesis (Figure 2). We quantified the association with
252 phylogeny for each trait by means of Blomberg's *K* statistic (Blomberg et al. 2003), to
253 assess whether traits conserved a phylogenetic signal; when *K* approaches 1 trait
254 evolution follows a mode of evolution that is consistent with Brownian motion, if $K > 1$
255 close relatives are more similar than expected under Brownian motion, while if $K < 1$
256 closely related species are less similar than expected (Blomberg et al. 2003). *K* has a
257 high type II error rate and a low power to detect a significant phylogenetic signal in
258 small phylogenies (less than 20 species; Blomberg et al. 2003; Münkemüller et al.
259 2012). Thus, we complemented the phylogenetic signal analysis with Abouheif's test
260 (Abouheif 1999; Pavoine et al. 2008). We used the R packages *phytools* (Revell 2012;
261 command "phylosig" with method="K") and *adephylo* (Jombart et al. 2010; command
262 "abouheif.moran" with method="oriAbouheif" and specifying the alternative hypothesis
263 as "greater") run under R version 3.1.2 (R Core Team 2014).
264
265 **Results**
266 Variation in the temperature finally reached in the heating experiments (i.e., asymptote)
267 was significantly explained by a mixed ANCOVA model (Table 4). The asymptotic
268 internal temperature of the specimens was positively related to subtle variations in the
269 air temperature during heating trials ($p << 0.001$), but it was not affected by the thoracic
270 volume of dung beetles. Radiation source and animal position also significantly affected
271 the asymptote ($p << 0.001$ and $p = 0.006$ respectively), with the magnitude effect of
272 heating source larger than that attributable to position (see Figure 3 for the partition of
273 variance in the main effects mixed model). The heat finally reached by the specimens

was higher under simulated sunlight conditions than under infrared radiation, and was higher when exposed dorsally than ventrally (Figure 4). The "source by position" interaction term attained significance (p=0.043), showing that the influence of animal position on the internal temperature finally reached was comparatively higher under sunlight conditions. The temperature reached by dung beetles when exposed dorsally was approximately 4 ºC higher in the case of simulated sun radiation than when they were heated with infrared radiation, being this difference only ca. 1.5 ºC higher when exposed ventrally to the two sources of radiation. Inter-specific differences did not reach significance and accounted for a low proportion of variance (Figure 3). The interaction terms including the species did not reach statistical significance, indicating that the above mentioned patterns were generalizable across species.

Variation in the increasing rate at the beginning of the heating experiments was also significantly explained by a mixed ANCOVA model (Table 4). Inter-specific differences did not reach significant values, accounting for a low proportion of variance (Figure 3). The starting heating rate was negatively related to the thoracic volume of beetles (p=0.003; large beetles heated more slowly) and was not affected by temperature variations during trials. Only animal body position had a significant influence on the heating rate (p<<0.001), while the source of radiation did not affect this parameter (Figure 4): beetles heated faster when exposed dorsally, independently of the source of radiation. None of the interaction terms reached significance, indicating that the above mentioned patterns were generalizable across species and experimental conditions.

There were no significant differences among species regarding the flightless condition: p=0.296 in the t-test for the heating rate, and p=0.860 for the asymptote (considering the species as the sample unit because the flightless condition is a constant within species; df=11 in both t-tests,).

The interspecific residual variation of the mixed ANCOVA model in the heating rate (i.e., after controlling for temperature experienced during each heating trial, the thoracic volume of beetles and the two radiation sources and two body positions) shows a Blomberg's K=0.99 (p=0.126). A similar result was obtained when analyzing the residual variation in the temperature finally reached in the heating experiments: Blomberg's K=0.90 (p=0.235). Phylogenetic signal was significant in the two traits examined using the Abouheif's test, with a positive autocorrelation describing the relation of cross-taxonomic trait variation to phylogeny; heating rate: C_{mean}=0.37, p=0.024; asymptotic temperature: C_{mean}=0.36, p=0.033.

Discussion

The interspecific variability in exoskeleton characteristics of the selected Geotrupidae species does not seem to be enough to generate contrasted thermal responses to heating independently of the radiation source. Neither species identity nor flightless condition significantly affected the thermal response of the exoskeleton. Although it is not possible to discard the existence of interspecific significant differences when a higher number of species and individuals are considered, our results suggest that the amount of these differences should be in any case very low, especially in the case of asymptotic temperatures. For example, the contribution of species identity *per se* to heating rate was approximately one-third of that attributable to body size *per se* (see Figure 3), and was similar to the amount related to the dorsal vs. ventral position. The amount of variance related to interspecific differences in the asymptote of body temperature was 1/7 - 1/8 of that accounted for by radiation source or animal position. Nevertheless, Abouheif's tests show significant results, indicating that related species resemble each other more than they resemble species drawn at random from the phylogenetic

hypothesis in Figure 2 (Blomberg and Garland 2002). Interspecific differences among the 13 studied Geotrupidae species appear to follow a mode of evolution that is not easily distinguishable from Brownian motion (Blomberg et al's. K approaches 1), in which the amount of differentiation among species increases monotonically with the time since they diverged. Brownian motion is what should be expected if selection is not acting on the trait (see Blomberg et al. 2003). However, to infer a process from such phylogenetic patterns is risky (Revell et al. 2008). Thus, the cuticule characteristics of different species belonging to lineages that diverged around 80 million years ago (Cunha et al. 2011) have not changed substantially such that they promote important changes in the measured heating parameters. Hence, it is highly probable that any observable variation in exoskeleton characteristics should be evolutionarily examined taking into account other functional properties that temperature control (Gorb 2013).

Beetle exoskeleton exerted a differential influence on asymptotic internal temperature and heating rate depending on whether the specimens were dorsally or ventrally exposed to the radiation sources. The smooth dorsal cuticle seems to facilitate acquiring higher internal temperatures, and at higher rates, than the ventral intricate surface. Interestingly, the dorsal cuticle also allowed a final higher internal temperature when exposed to simulated sun irradiance than to infrared radiation. These results suggest that the higher internal temperature reached when the dorsal surface of the beetle is submitted to simulated natural sunlight is probably due to the transmittance across the cuticle of non-infrared wavelengths. Thus, sun radiation should be the main heating source when beetles are dorsally exposed. Acquiring heat dorsally from natural sunlight should be a valuable adaptation considering that most part of the ca. 350 Geotrupidae species of dung beetles inhabit temperate-cold environments (Hanski and Cambefort 1991). On the other hand, the lower difference between ventral and dorsal

cuticle in the asymptotic internal temperatures when beetles are exposed to infrared radiation suggests that infrared wavelengths have a comparatively higher importance in the acquisition of heat from the ventral cuticle. This is to be expected in animals that spend much of their life buried, acquiring heat from the soil or from dung pats to be active.

These results are in agreement with the importance conferred many years ago to shorter wavelengths in explaining body temperature excess of insect species (Digby 1955; Tracy 1979), as well as with the mentioned relevance of infrared radiation in explaining insect thermal responses (Porter and Kearney 2009). The results provided by this study would constitute the first evidence supporting that the exoskeleton of the beetles acts differentially across the electromagnetic spectrum determining the internal body temperatures. This interesting finding suggests the existence of a kind of "passive physiology" imposed by the exoskeleton, where interspecific differences not related to the mere body size play a very minor role.

Acknowledgements

This paper was funded by the project CGL2011-25544 of the Spanish Ministry of Economía y Competitividad. Special thanks to Claire Jasinski for the English revision of the manuscript. We highly appreciate the detailed and valuable comments of the referees and the editor of this manuscript.

372 **Literature Cited**

373 Abouheif, E. 1999. A method for testing the assumption of phylogenetic independence
374 in comparative data. Evol Ecol Res 1:895–909.

375 Akamine M., K. Ishikawa, K. Maekawa, and M. Kon. 2011. The physical mechanism of
376 cuticular color in *Phelotrupes auratus* (Coleoptera, Geotrupidae). Entomol Sci
377 14:291-296.

378 Ball G.E. 1985. Characteristics and evolution of elytral sculpture in the tribe Galeritini
379 (Coleoptera : Carabidae). Quaest Entomol 21:349-367.

380 Bates D., M. Maechler, B. Bolker, and S. Walker. 2015. Fitting linear mixed-effects
381 models using lme4. J Stat Softw 67:1-48. R package version 1.1-7. http://cran.r-
382 project.org/web/packages/lme4/index.html.

383 Blomberg, S.P. & T. Garland 2002. Tempo and mode in evolution: phylogenetic inertia,
384 adaptation and comparative methods. J Evol Biol 15:899–910.

385 Blomberg S.P., T. Garland, and A.R. Ives. 2003 Testing for phylogenetic signal in
386 comparative data: behavioral traits are more labile. Evolution 57:717–745.

387 Chapman A.D. 2009. Numbers of living species in Australia and the world. Australian
388 Biodiversity Information Services, Toowoomba, Australia. Available at
389 http://www.environment.gov.au/node/13875.

390 Clusella Trullas S., J.H. van Wyk, and J.R. Spotila. 2007. Thermal melanism in
391 ectotherms. J Therm Biol 32:235-245.

392 Cunha R.L., J.R. Verdú, J.M. Lobo, and R. Zardoya. 2011. Ancient origin of endemic
393 Iberian earth-boring dung beetles (Geotrupidae). Mol Phylogenet Evol 59: 578-
394 586.

395 Darriba D., G.L. Taboada, R. Doallo, and D. Posada. 2012. jModelTest 2: more models,
396 new heuristics and parallel computing. Nat Methods 9: 772.

397 Davis A.L.V., D.J. Brink, C.H. Scholtz, L.C. Prinsloo, and C.M. Deschodt. 2008.
398 Functional implications of temperature-correlated colour polymorphism in an
399 iridescent, Scarabaeine dung beetle. Ecol Entomol 33:771-779.
400 Digby P.S.B. 1955. Factors affecting the temperature excess of insects in sunshine. J
401 Exp Biol 32:279–298.
402 Doberski J. and G. Walmesley. 2007. Microsculpture in UK ground beetles: Are there
403 patterns? Entomol Sci 10:425-428.
404 Drotz M.K., T. Brodin, and A.N. Nilsson. 2010. Multiple origins of elytral reticulation
405 modifications in the west Palaearctic *Agabus bipustulatus* complex (Coleoptera,
406 Dytiscidae). PLoS ONE 5:e9034.
407 Dubovskiy I.M., M.M.A. Whitten, V.Y. Kryukov, O.N. Yaroslavtseva, E.V. Grizanova,
408 C. Greig, K. Mukherjee, A. Vilcinskas, P.V. Mitkovets, V.V. Glupov, and T.M.
409 Butt. 2013. More than a colour change: insect melanism, disease resistance and
410 fecundity. Proc. R Soc B 280: 20130584.
411 Duncan F.D. 2002. The role of subelytral cavity in water loss in the flightless dung
412 beetle, *Circellium bacchus* (Coleoptera: Scarabaeinae). Eur J Entomol 99:253-
413 258.
414 Fedorka K.M., V. Lee, and W.E Witerhalter. 2013. Thermal environments shapes
415 cuticle melanism and melanin-based immunity in the ground cricket *Allonemobius*
416 *socius*. Evol Ecol 27:521-531.
417 Folmer O., M. Black, W. Hoeh, R. Lutz, and R. Vrijenhoek, R. 1994. DNA primers for
418 amplification of mitochondrial cytochrome c oxidase subunit I from diverse
419 metazoan invertebrates. Mol Mar Biol Biotechnol 3:294–299.
420 Gorb S.N. 2013. Insect-inspired technologies: insects as a source for Biomimetics. Pp.
421 241-264 in A. Vilcinskas, ed. Insect Biotechnology. Springer, The Netherlands:.

422 Gross J., E. Schmolz, and M. Hilker. 2004. Thermal adaptations of the leaf beetle
423 *Chrysomela lapponica* (Coleoptera: Chrysomelidae) to different climes of central
424 and northern Europe. Environ Entomol 33:799-806
425 Guindon S., J.F. Dufayard, V. Lefort, M. Anisimova, W. Hordijk, and O. Gascuel.
426 2010. New algorithms and methods to estimate maximum-likelihood phylogenies:
427 assessing the performance of PhyML 3.0. Syst Biol 59:307-321.
428 Gupta N.S. ed. 2011. Chitin. Formation and diagenesis. Dordrecht, Springer.
429 Hall, T.A. 1999. BioEdit: a user–friendly biological sequence alignment editor and
430 analysis program for Windows 95/98/NT. Nucleic Acids Symp Ser 41:95–98.
431 Hanski I. and Y. Cambefort. 1991. Dung Beetle Ecology. Princeton University Press,
432 New Jersey.
433 Harvey P.H. and A. Purvis. 1991. Comparative methods for explaining adaptations.
434 Nature 351:619-624.
435 Jombart T., F. Balloux and S. Dray 2010. adephylo: new tools for investigating the
436 phylogenetic signal in biological traits. Bioinformatics 26:1907–1909.
437 Kenward M.G., and J.H. Roger. 1997. Small sample inference for fixed effects from
438 restricted maximum likelihood. Biometrics 53:983-997.
439 Kinoshita S. 2008. Structural colors in the realm of nature. World Scientific Publishing,
440 Singapore.
441 Kuznetsova A., P.B. Brockhoff, and R.H.B. Christensen. 2014. lmerTest: Tests for
442 random and fixed effects for linear mixed effect models. R package version 2.0-
443 20. http://cran.r-project.org/web/packages/lmerTest/index.html
444 Lobo J.M., Y. Jiménez-Ruiz, E. Chehlarov, B. Guéorguiev, Y. Petrova, D. Král, M.A.
445 Alonso-Zarazaga, and J.R.Verdú. 2015. The classification and phylogenetic status
446 of *Jekelius* (*Reitterius*) *punctulatus* (Jekel, 1866) and *Jekelius* (*Jekelius*) *brullei*

(Jekel, 1866) (Coleoptera: Geotrupidae) using molecular data. Zootaxa 4040:187-203.

Mikhailov Y.E. 2001. Significance of colour polymorphism in mountain populations of abundant leaf beetles (Coleoptera: Chrysomelidae). Pirineos 156:57-68.

Münkemüller T., S. Lavergne, B. Bzeznik, S. Dray, T. Jombart, K. Schiffers, and W. Thuiller. 2012. How to measure and test phylogenetic signal. Methods Ecol Evol 3:743–756.

Pavoine S., S. Ollier, D. Pontier and D. Chessel. 2008. Testing for phylogenetic signal in phenotypic traits: new matrices of phylogenetic proximities. Theor Popul Biol 73:79–91.

Porter W.P. and M. Kearney. 2009. Colloquium papers: size, shape, and the thermal niche of endotherms. Proc Natl Acad Sci USA 106:19666–19672.

Pye J. 2010. The distribution of circularly polarized light reflection in the Scarabaeoidea (Coleoptera). Biol J Linn Soc 100:585-596.

R Core Team. 2014. R: A language and environment for statistical computing. R Foundation for Statistical Computing, Vienna, Austria. http://www.R-project.org/.

Rambaut A., M.A. Suchard, W. Xie, and A.J. Drummond. 2013. Tracer v1.6. Available from http://tree.bio.ed.ac.uk/software/tracer

Revell L.J. 2012. Phytools: an R package for phylogenetic comparative biology (and other things). Methods Ecol Evol 3:217-223. R package version 0.5-10. https://cran.r-project.org/web/packages/phytools/index.html

Revell L., L. Harmon, and D. Collar. 2008. Phylogenetic signal, evolutionary process, and rate. Syst Biol 57:591–601.

Rezende E.L. and J.A.F. Diniz-Filho. 2012. Phylogenetic analyses: comparing species to infer adaptations and physiological mechanisms. Compr Physiol 2:639–674.

Ronquist F., M. Teslenko, P. van der Mark, D.L. Ayres, A. Darling, S. Höhna, B. Larget, L. Liu, M.A. Suchard, and J.P. Huelsenbeck. 2012. Mrbayes 3.2: Efficient bayesian phylogenetic inference and model choice across a large model space. Syst Biol 61:539-542.

Simon C., F. Frati, A. Beckenbach, B. Crespi, H. Liu, and P. Flook. 1994. Evolution, weighting and phylogenetic utility of mitochondrial gene sequences and a compilation of conserved polymerase chain reaction primers. Ann Entomol Soc Am 87: 651-701.

Slifer E.H. 1953. The pattern of specialized heat-sensitive areas on the surface of the body of Acrididae (Orthoptera). II. The females. Trans Am Entomol Soc 79:69–97.

Schweiger A.H. and C. Beierkuhnlein. 2016. Size dependency in colour patterns of Western Palearctic carabids. Ecography 39:846–857.

Tracy C.R. 1979. Emissivity, a little-explored variable. Pp. 28-32 in E.H Burtt Jr, ed. The behavioral significance of color. Garland STPM Press, New York.

Umbers K.D.L., M.E. Herberstein, and J.S. Madin. 2013. Colour in insect thermoregulation: empirical and theoretical test in the colour-changing grasshopper, *Kosciuscola tristis*. J Insect Physiol 59:81-90.

Välimäki P., S.M. Kivelä, J. Raitanen, V.M. Pakanen, E. Vatka, M.I. Mäenpää, N. Keret, and T. Tammaru. 2015. Larval melanism in a geometrid moth: promoted neither by a thermal nor seasonal adaptation but desiccating environments. J Anim Ecol 84:817-828.

Verdú J.R., E. Galante, J.P. Lumaret, and F.J. Sañudo. 2004. Phylogenetic analysis of Geotrupidae (Coleoptera, Scarabaeoidea) based on larvae. Syst Entomol 29:509–523.

497 Villalba, S., J.M. Lobo, F. Martín-Piera, and R. Zardoya. 2002. Phylogenetic
498 relationships of Iberian dung beetles (Coleoptera: Scarabaeinae): insights on the
499 evolution of nesting behavior. J Mol Evol 55:116-126.
500 Zeuss D., R. Brandl, M. Brändle, C. Rahbek, and S. Brunzel. 2014. Global warming
501 favours light-coloured insects in Europe. Nature Comm 5:3874.
502

Table 1.- Flightless character and geographical distribution of the studied Geotrupidae species, as well as thoracic volume (mm^3) of each one of the two treated individuals and the locality in which were collected.

Species	Flightless	Distribution	thoracic volume	Origin
Jekelius albarracinus	yes	Iberian	325	Beceite, Teruel (Spain)
			284	Beceite, Teruel (Spain)
Jekelius hispanus	yes	Iberian	287	Doñana National Park (Spain)
			254	Doñana National Park (Spain)
Thorectes armifrons	yes	Moroccan	338	Middle Atlas (Morroco)
			246	Middle Atlas (Morroco)
Thorectes lusitanicus	yes	Iberian	569	Los Acornocales, Cadiz (Spain)
			283	Sª Aljibe, Cadiz (Spain)
Typhaeus typhoeus	not	European	407	Pto Canencia, Madrid (Spain)
			374	El Pardo, Madrid (Spain)
Chelotrupes momus	yes	Iberian	495	Doñana National Park (Spain)
			409	Tarifa, Cadiz (Spain)
Silphotrupes escorialensis	yes	Iberian	246	El Escorial, Madrid (Spain)
			220	Sª Gredos, Avila (Spain)
Trypocopris vernalis	not	Euro-Caucasian	473	Rhodope Mountains (Bulgaria)
			431	La Viale Lozère (France)
Sericotrupes niger	not	Western Palaearctic	672	Middle Atlas (Morroco)
			489	Villanueva del Fresno, Badajoz (Spain)
Geotrupes mutator	not	Euro-Caucasian	568	Sª Gredos, Avila (Spain)
			313	Pto. Cardoso, Madrid (Spain)
Geotrupes stercorarius	not	Holarctic	735	Pto Quesera, Madrid (Spain)
			701	Somiedo, Asturias (Spain)
Anoplotrupes stercorosus	not	Western Palaearctic	1036	Puymorens (Andorra)
			400	Rhodope Mountains (Bulgaria)
Ceratophyus hoffmannssegi	not	Ibero-Maghrebian	807	Las Matas, Madrid (Spain)
			1137	Doñana National Park (Spain)

Table 2.- Mean and standard errors (se) of the increasing rate of temperature at the beginning of heating trials (Heating rate) and body temperature finally reached in heating experiments (Asymptote) for the 13 studied species under two sources of radiation (infrared vs. solar radiance) and two body positions (dorsal vs. ventral).

			Heating rate		Asymptote	
Species	radiation of source	body position	mean	se	mean	se
Anoplotrupes stercorosus	infrared	dorsal	0.029	0.0077	49.49	2.63
Anoplotrupes stercorosus	infrared	ventral	0.025	0.0059	43.46	2.01
Anoplotrupes stercorosus	solar radiance	dorsal	0.024	0.0071	48.24	2.16
Anoplotrupes stercorosus	solar radiance	ventral	0.027	0.0083	49.02	3.96
Ceratophyus hoffmannseggi	infrared	dorsal	0.023	0.0020	53.38	8.21
Ceratophyus hoffmannseggi	infrared	ventral	0.014	0.0068	44.43	0.93
Ceratophyus hoffmannseggi	solar radiance	dorsal	0.023	0.0051	50.79	2.09
Ceratophyus hoffmannseggi	solar radiance	ventral	0.016	0.0083	48.63	0.65
Geotrupes mutator	infrared	dorsal	0.033	0.0045	46.42	5.62
Geotrupes mutator	infrared	ventral	0.025	0.0059	43.02	0.93
Geotrupes mutator	solar radiance	dorsal	0.027	0.0080	47.14	3.59
Geotrupes mutator	solar radiance	ventral	0.028	0.0085	42.53	0.43
Geotrupes stercorarius	infrared	dorsal	0.020	0.0029	50.70	5.95
Geotrupes stercorarius	infrared	ventral	0.017	0.0011	44.63	0.29
Geotrupes stercorarius	solar radiance	dorsal	0.016	0.0000	51.80	3.81
Geotrupes stercorarius	solar radiance	ventral	0.017	0.0017	46.94	3.73
Jekelius albarracinus	infrared	dorsal	0.017	0.0062	42.43	2.69
Jekelius albarracinus	infrared	ventral	0.021	0.0011	39.89	2.28
Jekelius albarracinus	solar radiance	dorsal	0.021	0.0024	50.37	2.65
Jekelius albarracinus	solar radiance	ventral	0.019	0.0049	44.16	0.24
Jekelius hispanus	infrared	dorsal	0.022	0.0030	40.32	3.29
Jekelius hispanus	infrared	ventral	0.024	0.0001	41.20	4.09
Jekelius hispanus	solar radiance	dorsal	0.024	0.0003	48.74	1.65
Jekelius hispanus	solar radiance	ventral	0.023	0.0015	42.44	0.01
Silphotrupes escorialensis	infrared	dorsal	0.030	0.0030	43.33	5.01
Silphotrupes escorialensis	infrared	ventral	0.027	0.0038	40.57	4.21
Silphotrupes escorialensis	solar radiance	dorsal	0.027	0.0014	49.82	2.38
Silphotrupes escorialensis	solar radiance	ventral	0.023	0.0057	41.85	1.20
Sericotrupes niger	infrared	dorsal	0.023	0.0068	48.84	0.06
Sericotrupes niger	infrared	ventral	0.022	0.0041	47.45	5.50
Sericotrupes niger	solar radiance	dorsal	0.019	0.0026	50.39	0.70
Sericotrupes niger	solar radiance	ventral	0.020	0.0029	40.06	3.14
Thorectes armifrons	infrared	dorsal	0.022	0.0092	40.04	3.37
Thorectes armifrons	infrared	ventral	0.024	0.0050	42.96	4.23
Thorectes armifrons	solar radiance	dorsal	0.024	0.0045	45.57	2.18
Thorectes armifrons	solar radiance	ventral	0.021	0.0064	43.27	0.21
Thorectes lusitanicus	infrared	dorsal	0.022	0.0101	40.24	4.33
Thorectes lusitanicus	infrared	ventral	0.021	0.0113	37.96	1.54

Thorectes lusitanicus	solar radiance	dorsal	0.023	0.0143	49.56	3.79
Thorectes lusitanicus	solar radiance	ventral	0.020	0.0119	38.14	2.12
Chelotrupes momus	infrared	dorsal	0.030	0.0030	44.17	0.47
Chelotrupes momus	infrared	ventral	0.025	0.0050	39.18	2.57
Chelotrupes momus	solar radiance	dorsal	0.029	0.0055	47.08	3.85
Chelotrupes momus	solar radiance	ventral	0.025	0.0033	45.93	2.05
Typhaeus typhoeus	infrared	dorsal	0.022	0.0020	37.91	1.77
Typhaeus typhoeus	infrared	ventral	0.018	0.0014	39.21	0.41
Typhaeus typhoeus	solar radiance	dorsal	0.017	0.0020	44.08	0.37
Typhaeus typhoeus	solar radiance	ventral	0.019	0.0007	40.00	4.43
Trypocopris vernalis	infrared	dorsal	0.021	0.0051	40.54	0.52
Trypocopris vernalis	infrared	ventral	0.021	0.0041	43.42	7.22
Trypocopris vernalis	solar radiance	dorsal	0.021	0.0042	43.81	1.50
Trypocopris vernalis	solar radiance	ventral	0.019	0.0024	45.23	1.25

Table 3.- List of species used in this study, collection locality and accession number for mitochondrial gene fragments (*: this study; **: Lobo *et al.*, 2015; ***: Cunha *et al*., 2011).

Species	Locality	Accession number COI-COII	
Jekelius albarracinus (Wagner, 1928)	Spain. Albacete: El Ballestero	GU984604***	KP657665**
Jekelius hispanus (Reitter, 1893)	Spain. Huelva: Doñana	GU984628***	KP657670**
Thorectes armifrons (Reitter, 1892)	Morroco: Ifrane		KP657673**
Thorectes lusitanicus (Jekel, 1866)	Spain. Cádiz: Los Alcornocales		KP657674**
Typhaeus typhoeus (Linnaeus, 1758)	Spain. Ávila: El Tiemblo	GU984619***	LT560390*
Chelotrupes momus (Olivier, 1789)	Spain. Huelva: Doñana	GU984620***	LT560391*
Silphotrupes escorialensis (Jekel, 1866)	Spain. Ávila: El Barraco		LT560384*
Trypocopris vernalis (Linnaeus, 1758)	Bulgaria. Vitosha Mts		LT560385*
Sericotrupes niger (Marsham, 1802)	Morroco: Moyen Atlas	GU984609***	LT560392*
Geotrupes mutator (Marsham, 1802)	Spain. Ávila: El Tiemblo	GU984606***	LT560393*
Geotrupes stercorarius (Linnaeus, 1758)	Spain. León: Puerto Ancares	GU984634***	LT560394*
Anoplotrupes stercorosus (Scriba, 1791)	Bulgaria: Belasitsa Mountain		LT560386*
Ceratophyus hoffmannseggi Fairmaire, 1856	Spain. Huelva: Doñana		LT560387*
Lethrus elephas Reitter, 1890	Greece: Tsotili Village		LT560388*
Lethrus perun Král & Hillert, 2013	Bulgaria: Drangovo Village		LT560389*

Table 4.- Results of general mixed ANCOVA GLMM models analyzing the internal body temperature finally reached in heating experiments (asymptote) by the studied beetles, and the increasing rate of temperature at the beginning of heating trials. The models analyze two different individuals of the 13 studied species under two sources of radiation (infrared vs. visible light) and two body positions (dorsal vs. ventral). Denominator degrees of freedom follow the Kenward-Roger approach to GLMM and have been rounded to the nearest unit. For more details see the Methods section.

	Asymptote			Starting heating rate		
	df	*F*	p	df	*F*	p
Thoracic volume	1, 13	0.05	0.829	1, 16	12.42	0.003
Temperature	1, 164	23.49	<<0.001	1, 50	0.1	0.75
Species	12, 12	1.17	0.392	12, 12	0.94	0.543
Source of	1, 21	29.86	<<0.001	1, 35	2.11	0.155
Body position	1, 13	10.65	0.006	1, 13	17.54	<0.001
Species x Source	12, 13	0.55	0.847	12, 13	0.57	0.828
Species x	12, 13	0.51	0.872	12, 12	1.79	0.161
Source x	1, 13	5.02	0.043	1, 13	0.19	0.674
Full interaction	12, 13	1.59	0.208	12, 13	1.29	0.327

Figure legends

Figure 1.- Representation of the factorial design and the effects tested (arrows) considering two sources of radiation (solar radiance and infrared; SR and IF, respectively) and two body positions (dorsal and ventral, D and V, respectively) on the heating response of thirteen Geotrupidae dung beetle species. The trials were carried out in two different specimens belonging to each species.

Figure 2.- Phylogenetic relationships of the studied Geotrupidae species based on maximum likelihood (ML) and Bayesian inference analysis (both procedures generate similar trees) using mitochondrial (COI, COII, tRNA-Leu) genes and the GTR + I + G evolutionary model. Numbers at nodes correspond to ML bootstrap proportions (BP) (first number) and Bayesian posterior probabilities (BPP) (second number). Only BP and BPP values above 50% and 90%, respectively, are represented.

Figure 3.- Partition of variance in asymptote of the temperature finally reached by the studied specimens and heating rate at the beginning of the trials among five different effects: size of individual beetles (thoracic pseudo-volume), subtle random variations in air temperature during heating trials (temperature), source of radiation (infrared vs. natural sunlight), body position (dorsal vs. ventral) and species identity (13 Geotrupidae dung beetle species). R^2: marginal proportion of the variance explained by the fixed factors in the GLMM without interaction terms.

Figure 4. Effect of the source of radiation and the body position of the studied specimens on the asymptote of the temperature finally reached and the heating rate at the beginning of the heating trials. Values are adjusted means ($\pm$ one SE) controlling for the effect of inter-individual differences in the thoracic volume of dung beetles and subtle, random, variations in temperature during trials. Sample size is two different individuals in 13 species of Geotrupidae.

Figure 1.

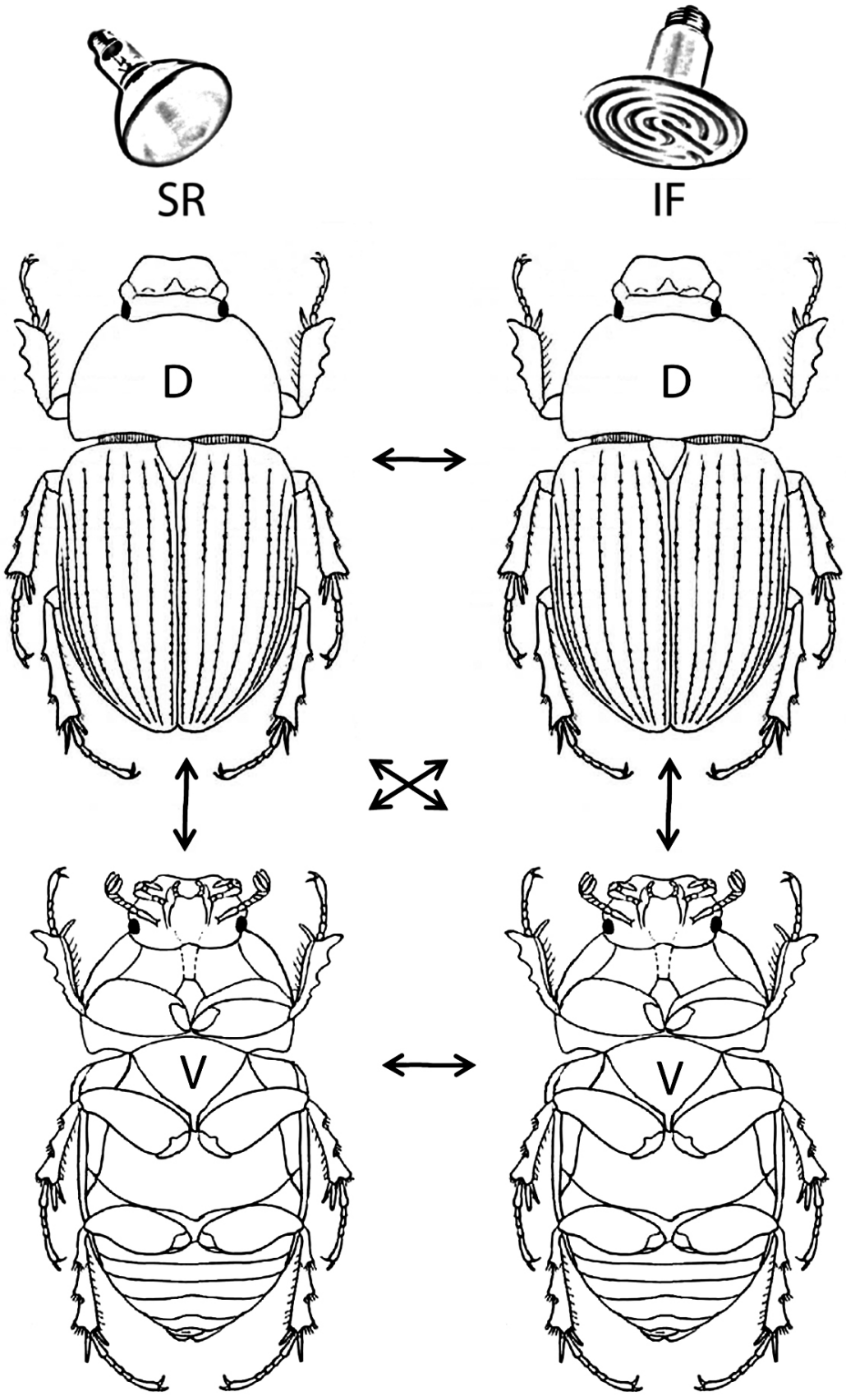

Figure 2.

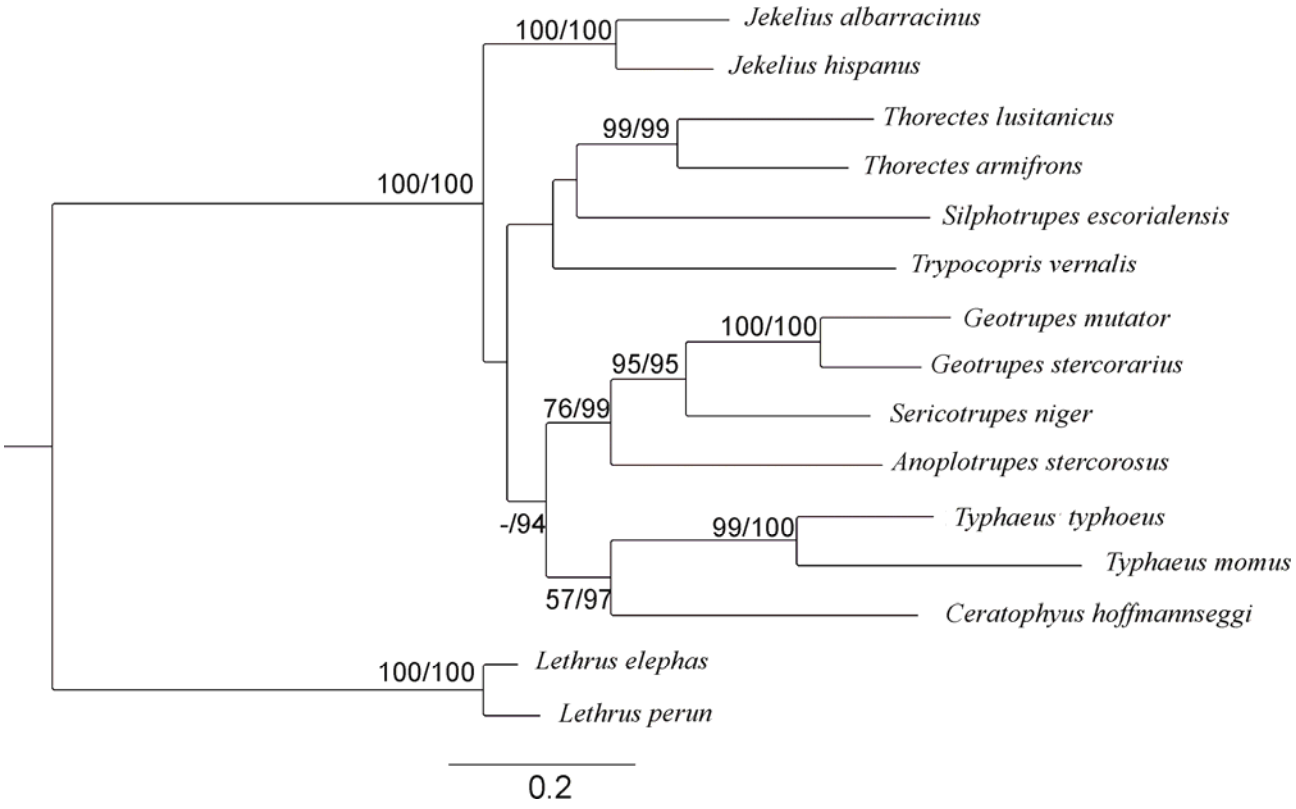
100/100
Jekelius albarracinus
Jekelius hispanus
99/99
Thorectes lusitanicus
Thorectes armifrons
100/100
Silphotrupes escorialensis
Trypocopris vernalis
100/100
Geotrupes mutator
95/95
Geotrupes stercorarius
76/99
Sericotrupes niger
Anoplotrupes stercorosus
-/94
99/100
Typhaeus typhoeus
Typhaeus momus
57/97
Ceratophyus hoffmannseggi
100/100
Lethrus elephas
Lethrus perun
0.2

Figure 3.

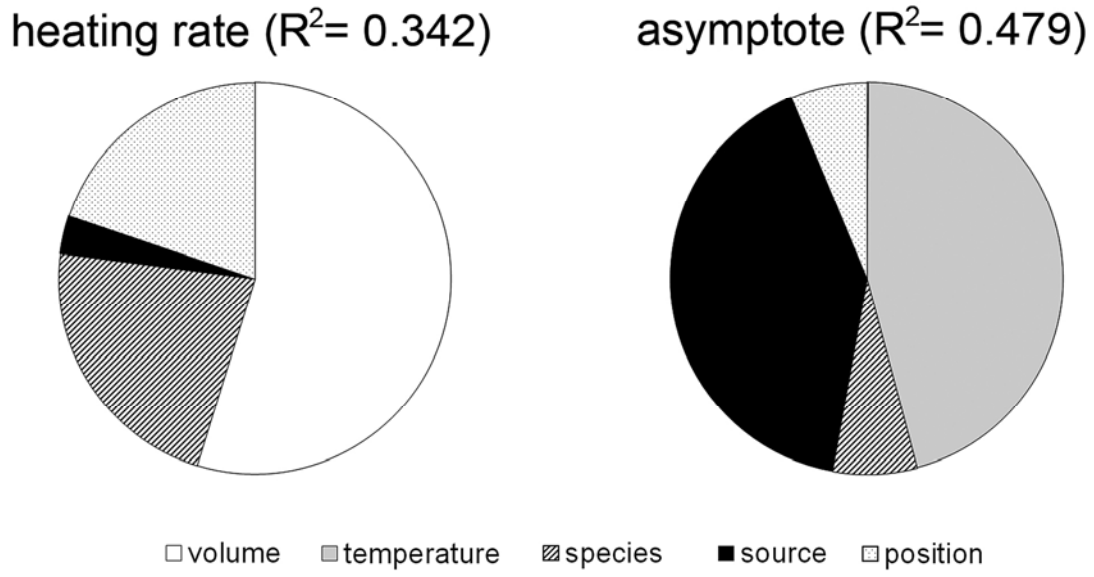
heating rate (R^2= 0.342)
asymptote (R^2= 0.479)
volume
temperature
species
source
position

Figure 4.

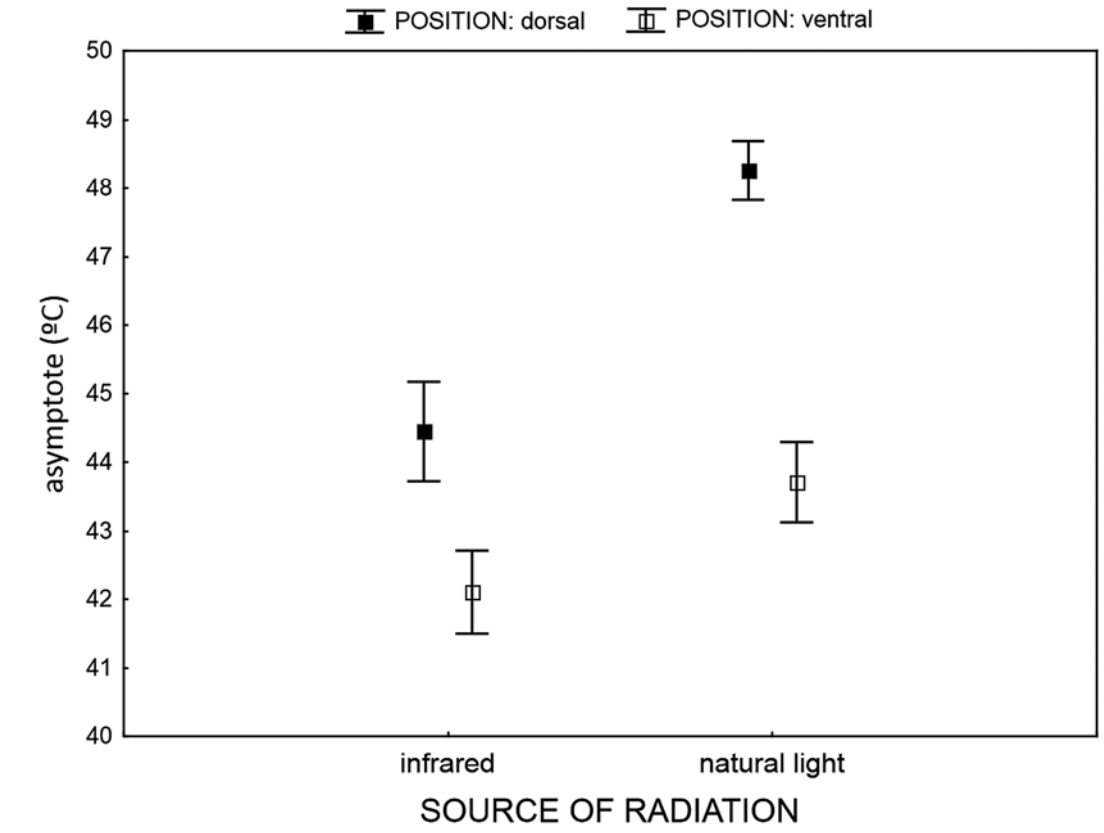
POSITION: dorsal
POSITION: ventral
asymptote (ºC)
50
49
48
47
46
45
44
43
42
41
40
infrared
natural light
SOURCE OF RADIATION

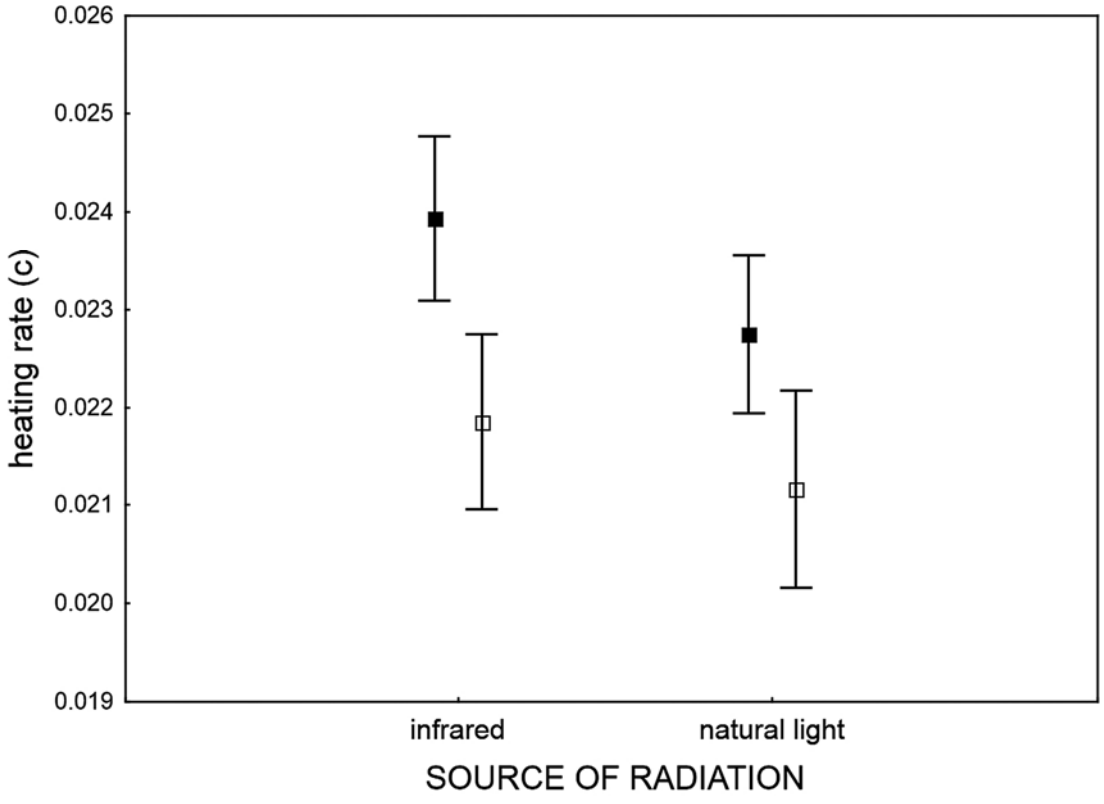
heating rate (c)
0.026
0.025
0.024
0.023
0.022
0.021
0.020
0.019
infrared
natural light
SOURCE OF RADIATION